Title
CROSS-HOLE ACOUSTIC SURVEYING IN BASALT

Authors
Rezowalli, J.J.
King, M.S.
Myer, L.R.

Publication Date
1984

LBL-17314 c2
Preprint

Lawrence Berkeley Laboratory
UNIVERSITY OF CALIFORNIA

EARTH SCIENCES DIVISION

To be published in the International Journal of Rock Mechanics Mining Sciences and Geomechanics Abstracts

CROSS-HOLE ACOUSTIC SURVEYING IN BASALT

J.J. Rezowalli, M.S. King, and L.R. Myer

January 1984

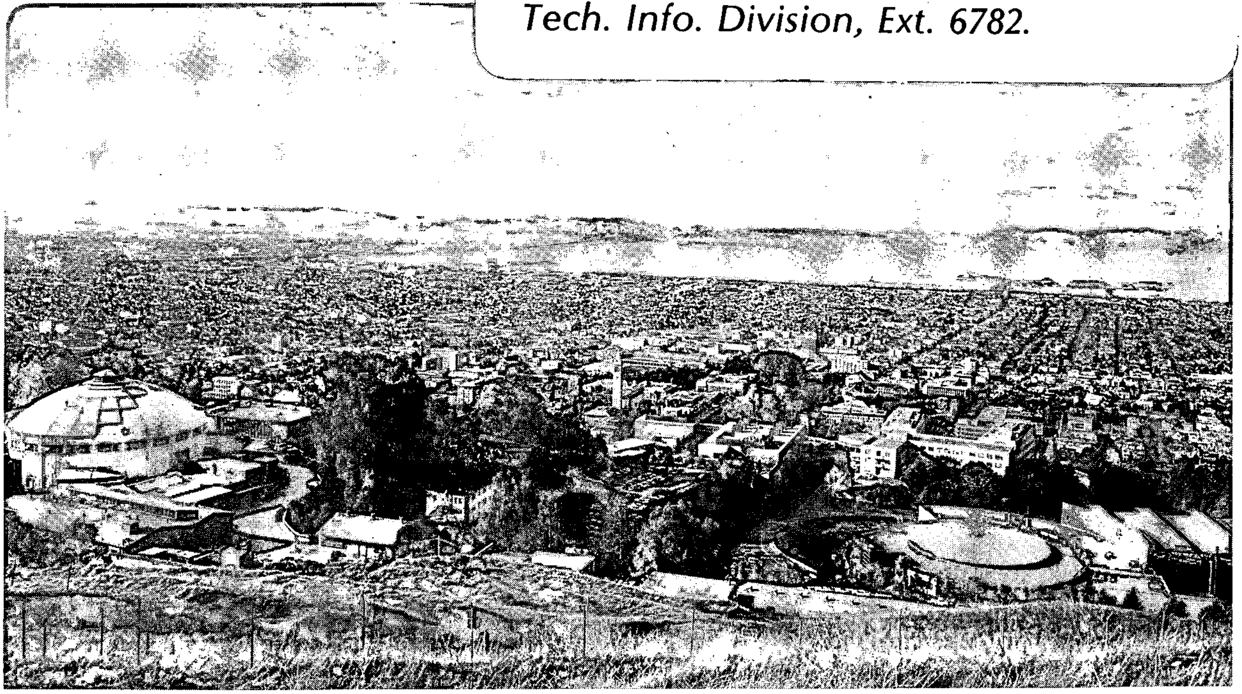

Prepared for the U.S. Department of Energy under Contract DE-AC03-76SF00098

LBL-17314 c.2

LBL-17314

Technical Note:

Cross-hole Acoustic Surveying in Basalt

by

J.J. Rezowalli, M.S. King, and L.R. Myer
Earth Sciences Division, Lawrence Berkeley Laboratory
University of California, Berkeley, CA 94720

Accepted for publication by the
Internat. J. Rock Mech. Min. Sci.
& Geomech. Abstr.

January 1984

This paper was prepared under U.S. Department of Energy Contract No. DE-AC03-76SF00098 with Lawrence Berkeley Laboratory.

INTRODUCTION

The _in situ_ assessment of geomechanical characteristics of rock masses is an essential prerequisite to the design and analysis of structures, both on the surface and underground. A particular _in situ_ investigative technique that continues to show promise for this purpose is the cross-hole higher-frequency acoustic method.

In recent years cross-hole acoustic techniques have been employed in a variety of geomechanical applications. Price _et al_ [1] incorporated results of cross-hole measurements in the design of a rock-bolt pattern intended to stabilize a rock mass. Kujundzic _et al_ [2] demonstrated the correlation between cross-hole velocity measurements and the compressive stress distribution around a tunnel excavated at depth. O'Donoghue _et al_ [3] employed the technique to investigate the spatial variation in rock properties encountered during tunneling, and to assess the degree of damage in the rock mass caused by different excavation techniques. Using the cross-hole technique, McCann _et al_ [4] delineated interfaces between different strata and detected localized irregular features. Auld [5] used cross-hole measurements to evaluate the elastic properties of a rock mass. Paulsson and King [6] studied the changes in cross-hole compressional and shear-wave velocities resulting from thermal cycling in a granitic rock mass. McKenzie _et al_ [7] and Gladwin [8] employed cross-hole ultrasonic measurements to characterize the degree of fracturing in a rock mass, and to monitor stress changes in the pillars of underground mines. Recently, Wong _et al_ [9] have reported acoustic cross-hole measurements in crystalline rocks, that were used to infer changes in lithology and to trace fracture zones between boreholes.

The purpose of this technical note is to present preliminary results of a series of cross-hole acoustic measurements performed in a tunnel situated in a basaltic rock mass. The tunnel, at a subsurface depth of 46 m, was excavated by conventional drill-and-blast techniques. Located well above the water table, the rock mass is characterized as dense basalt with a jointing structure of 0.15 to 0.36 m thick vertical columns cut by low-angle cross joints.

The objectives of the test program were: first, to evaluate *in situ* dynamic elastic properties, and to assess their spatial variation around the opening; second, to evaluate the extent of blast damage around the opening; and third, to assess the spatial variation of jointing and fracturing around the opening. Analysis of the data included an evaluation of the velocities and frequency spectra of compressional and shear waves transmitted through the rock.

EXPERIMENTAL PROCEDURES

Acoustic velocity measurements were made between four 76 mm diameter, horizontal boreholes diamond-drilled into the wall of the tunnel. Approximately 550 acoustic measurements were made in vertical, parallel planes at different distances from the face between six pairs of the four boreholes, as indicated in Fig. 1. In the first 1.5 m from the tunnel face, the acoustic measurements were made at 0.15 m intervals; from 2 m to 11 m from the face, the measurements were made at 1 m intervals. The shorter interval spacings were intended to characterize more carefully the extent of the expected zone of blast damage adjacent to the tunnel.

The field system employed is shown in diagrammatic form in Fig. 2. It is based essentially on that used in a similar research program conducted earlier in a granitic rock mass in Sweden [6]. Repetitive pulses of compressional (P) and shear (S) waves in the frequency range 1 kHz to 100 kHz were propagated from the transmitter sonde, situated in one borehole, through the rock mass to the receiver sonde, situated in a second borehole. The P- and S-wave transmitter and receiver transducers are broadband ceramic-steel sandwiches, with a center frequency of approximately 80 kHz. The sondes were clamped hydraulically to the borehole wall to ensure repeatable acoustic contact. The received P- and S-wave signals were preamplified in the sonde and transmitted to the surface, where they were further amplified and bandpass filtered in the frequency range 500 Hz to 100 kHz. The complete P- and S-waveforms were digitized by a digital oscilloscope with a 1MHz sampling rate, and stored on floppy discs. An auxiliary analog tape recorder, with a 62 kHz bandwidth, may be employed where the signals are of such poor quality that signal enhancement by stacking is required.

The digitized P- and S-waveforms were analyzed to determine the arrival times of P- and S-wave pulses, so that the velocities V_P and V_S could be determined using the distances between the pairs of boreholes calculated from survey data. The arrival times were corrected for the delay times of the transducer holders by clamping the sondes in an aluminum calibration block. The digitized waveforms were also subjected to Fast Fourier Transforms (FFT), and their amplitude spectra in the frequency domain were studied.

RESULTS AND DISCUSSION

Preliminary results of the test program are shown in Figs. 3-8. In Figs. 3 and 4 are shown the compressional-wave velocities measured between boreholes 1 and 2 vertically, 3 and 4 horizontally, 2 and 4 diagonally, and 1 and 4 diagonally, as a function of distance of the plane of measurement from the tunnel face. Figs. 5 and 6 show the shear-wave velocities measured in the same manner. Experimental errors ensuing from possible errors in the arrival times and survey data are indicated by error bars. In the case of a few S-wave arrivals, however, the errors could be larger, because of difficulties in recognizing the correct arrival buried in earlier arrivals of mode-converted P-waves. Using the equations of the classical theory of elasticity and an average measured density of 2848 kg/m^3, the elastic modulus and Poisson's ratio were calculated and plotted as shown in Figs. 7 and 8. Comparison of the data plotted in Figs. 3-8 indicates that the acoustic velocities and elastic properties for the diagonal paths (between boreholes 2 and 4, and 1 and 4) tend to lie between the upper and lower limits established by measurements made in the vertical (between boreholes 1 and 3) and horizontal (between boreholes 3 and 4) directions.

Figs. 3-8 show that there are considerable reductions in V_P, V_S, and elastic modulus at distances less than 2 m from the face: up to 55% to 65% in magnitude for the velocities. Clearly these low acoustic velocities and elastic moduli are associated with blast damage adjacent to the tunnel. However, the calculated dynamic values of Poisson's ratio appeared relatively insensitive to the degree of jointing or fracturing. At 2 m from the face and beyond, the velocities measured in the vertical direction indicate almost constant values, with a tendency for a slight decrease in magnitude at distances greater than 7 m. This behavior may well be due to a vertical stress concentration present around the tunnel. The velocities in the horizontal direction at 2 m from the face and beyond appear erratic, but show a general tendency to increase as a function of distance from the face. They remain, however, some 15% in value lower than the corresponding velocities measured in the vertical direction. Near the face, values of V_P and V_S in the horizontal direction were approximately 30% lower in value than those measured in the vertical direction. Velocities measured along the diagonal paths are seen to lie between those measured along the vertical and horizontal paths.

Results of the FFT analysis indicate that there is a considerable difference in frequency content of the received P- and S-wave signals between those propagating along horizontal and those along vertical paths, and between those measured in planes lying close to the face and those in planes well behind the face. Near the face, both P- and S-wave amplitude spectra tend to peak at approximately 3 kHz or less. Further away from the face, at distances greater than approximately 2 m, the amplitude spectra for P- and S-waves propagating along vertical paths tend to peak at 20 kHz or more, and those along horizontal paths at 5 kHz or less. The amplitude spectra for P- and S-waves propagating along diagonal paths again tend to fall between the limits provided by those propagating vertically and horizontally.

The velocity and frequency data correspond to a model of a jointed rock mass in which the joints intersected in the vertical direction are fewer and probably tighter than those intersected in the horizontal direction. The nature of the columnar-jointed rock mass in which the test program was conducted supports this model. A convenient model for further study of the elastic-wave propagation in a regularly-jointed rock mass, with idealized areas of contacts for the joints, has been suggested by White [10]. Further analyses of the velocity and frequency data, in conjunction with studies of the borehole core logs and ultrasonic measurements performed on specimens of core recovered from the boreholes, are intended to provide the basis for a quantitative model of the rock mass.

CONCLUSIONS

1. The acoustic velocity and attenuation data are clearly indicative of an anisotropic, jointed rock mass, with a greater intensity of jointing in the horizontal than the vertical direction.

2. Low acoustic velocities are indicative of blast damage, and of zones of intense jointing or fracturing. The same trend is seen also in the values of dynamic elastic modulus. The dynamic Poisson's ratio, however, appears to be relatively insensitive to the degree of jointing or fracturing.

3. Preliminary analyses of the frequency data show that the attenuation of elastic waves is also indicative of blast damage and the intensity of jointing and fracturing. Further analyses of the frequency data are clearly required.

ACKNOWLEDGEMENT

This paper was prepared under U.S. Department of Energy Contract No. DE-AC03-76SF00098 with Lawrence Berkeley Laboratory.

REFERENCES

1. Price D. G., Malone A. W. & Knill, J. L. The application of seismic methods in the design of rock bolt systems. Proc. I Int. Congr. IAEG, Paris, 2, pp. 740-752 (1970).

2. Kujundzic B., Jovanovic L. & Radosavljevic Z. A pressure tunnel lining using high-pressure grouting (in French). Proceedings of the 2nd Congress International Society for Rock Mechanics, Belgrade, 2, pp. 867-881 (1970).

3. O'Donoghue L. B. & O'Flaherty R. M. The underground works in Turlough Hill; Part I. Water Power, pp. 5-12, (1974, January).

4. McCann D. M., Grainger P. & McCann C. Inter-borehole acoustic measurements and their use in engineering geology. Geophys. Prospect. 23, pp. 50-69 (1975).

5. Auld B. Cross-hole and down-hole V_S by mechanical impulse. J. Geotech. Engng. Div. Am. Soc. civ. Engrs. 103, GT 12, pp. 1381-1398 (1977).

6. Paulsson B. N. P. & King M. S. Between-hole acoustic surveying and monitoring of a granitic rock mass. Int. J. Rock Mech. Min. Sci. & Geomech. Abstr. 17, pp. 371-376 (1980).

7. McKenzie C. K., Stacey G. P. & Gladwin M. T. Ultrasonic characteristics of a rock mass. Int. J. Rock Mech. Min. Sci. & Geomech. Abstr. 19, pp. 25-30 (1982).

8. Gladwin M. T. Ultrasonic stress monitoring in underground mining. Int. J. Rock Mech. Min. Sci. & Geomech. Abstr. 19, pp. 221-228 (1982).

9. Wong J., Hurley P. & West G. F. Cross-hole seismology and seismic imaging in crystalline rocks. Geophys. Res. Let. 10, pp. 686-689 (1983).

10. White J. E. Underground Sound: Application of Seismic Waves, pp. 78-81. Elsevier, New York.

FIGURE CAPTIONS

Figure 1. Layout of boreholes in tunnel wall.

Figure 2. Block diagram of cross-hole acoustic system.

Figure 3. Compressional-wave velocity in vertical and horizontal directions between boreholes.

Figure 4. Compressional-wave velocity in diagonal directions between boreholes.

Figure 5. Shear-wave velocity in vertical and horizontal directions between boreholes.

Figure 6. Shear-wave velocity in diagonal directions between boreholes.

Figure 7. Dynamic elastic modulus and Poisson's ratio in vertical and horizontal directions.

Figure 8. Dynamic elastic modulus and Poisson's ratio in diagonal directions.

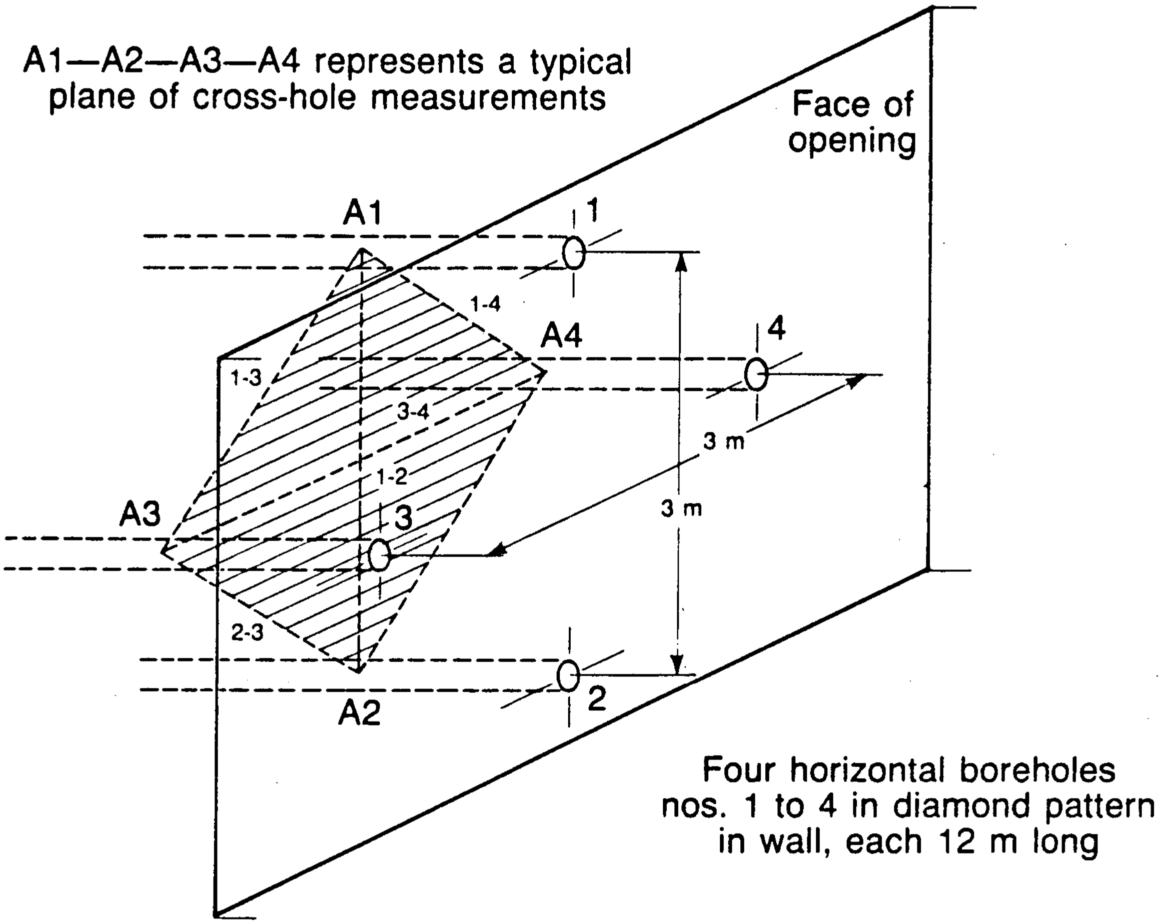
A1—A2—A3—A4 represents a typical plane of cross-hole measurements
Face of opening
A1
1
1-4
A4
4
1-3
3-4
3 m
1-2
3 m
A3
3
2-3
2
A2
Four horizontal boreholes nos. 1 to 4 in diamond pattern in wall, each 12 m long

Figure 1

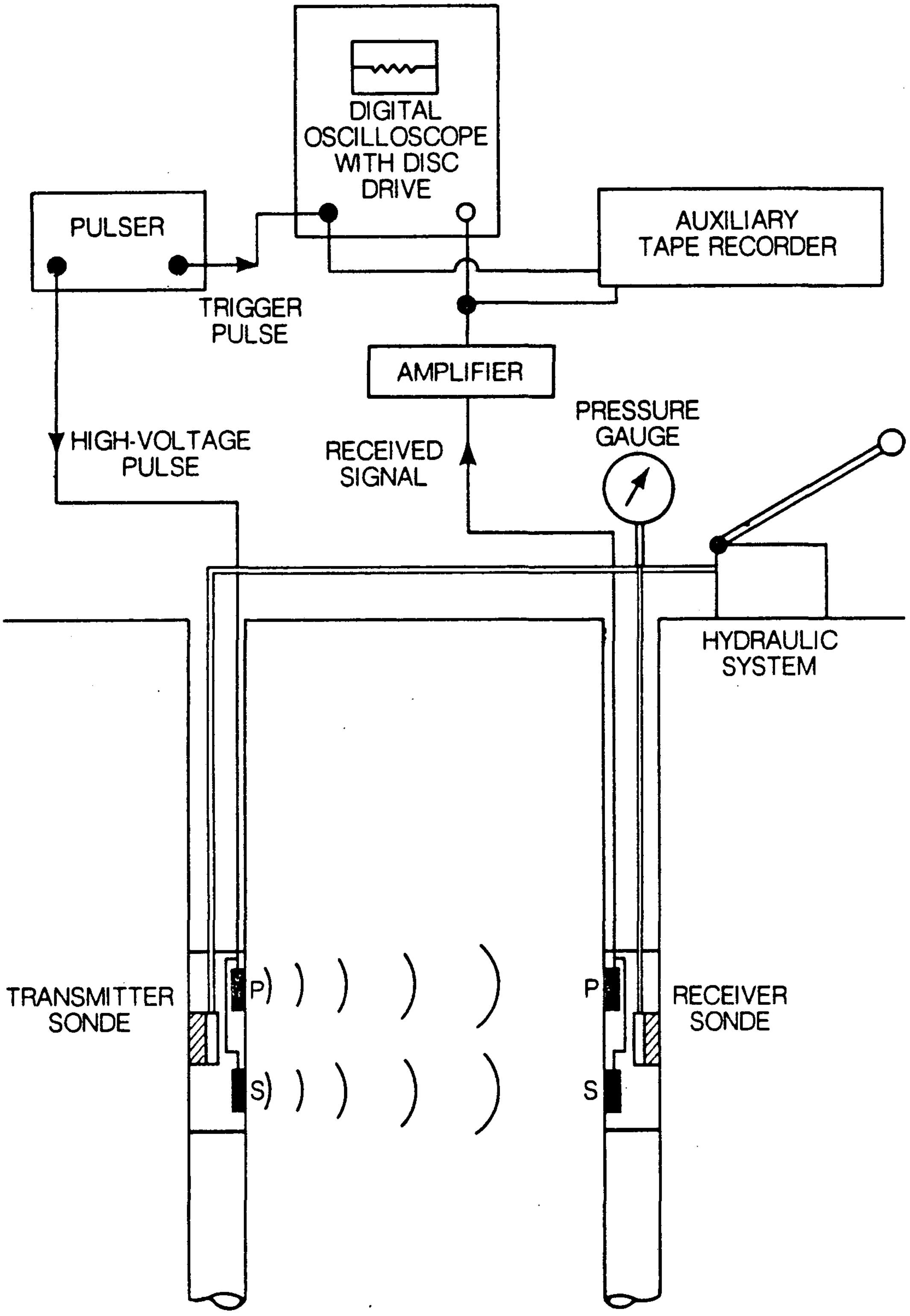
DIGITAL OSCILLOSCOPE WITH DISC DRIVE
PULSER
AUXILIARY TAPE RECORDER
TRIGGER PULSE
AMPLIFIER
PRESSURE GAUGE
HIGH-VOLTAGE PULSE
RECEIVED SIGNAL
HYDRAULIC SYSTEM
TRANSMITTER SONDE
P
S
P
S
RECEIVER SONDE

Figure 2

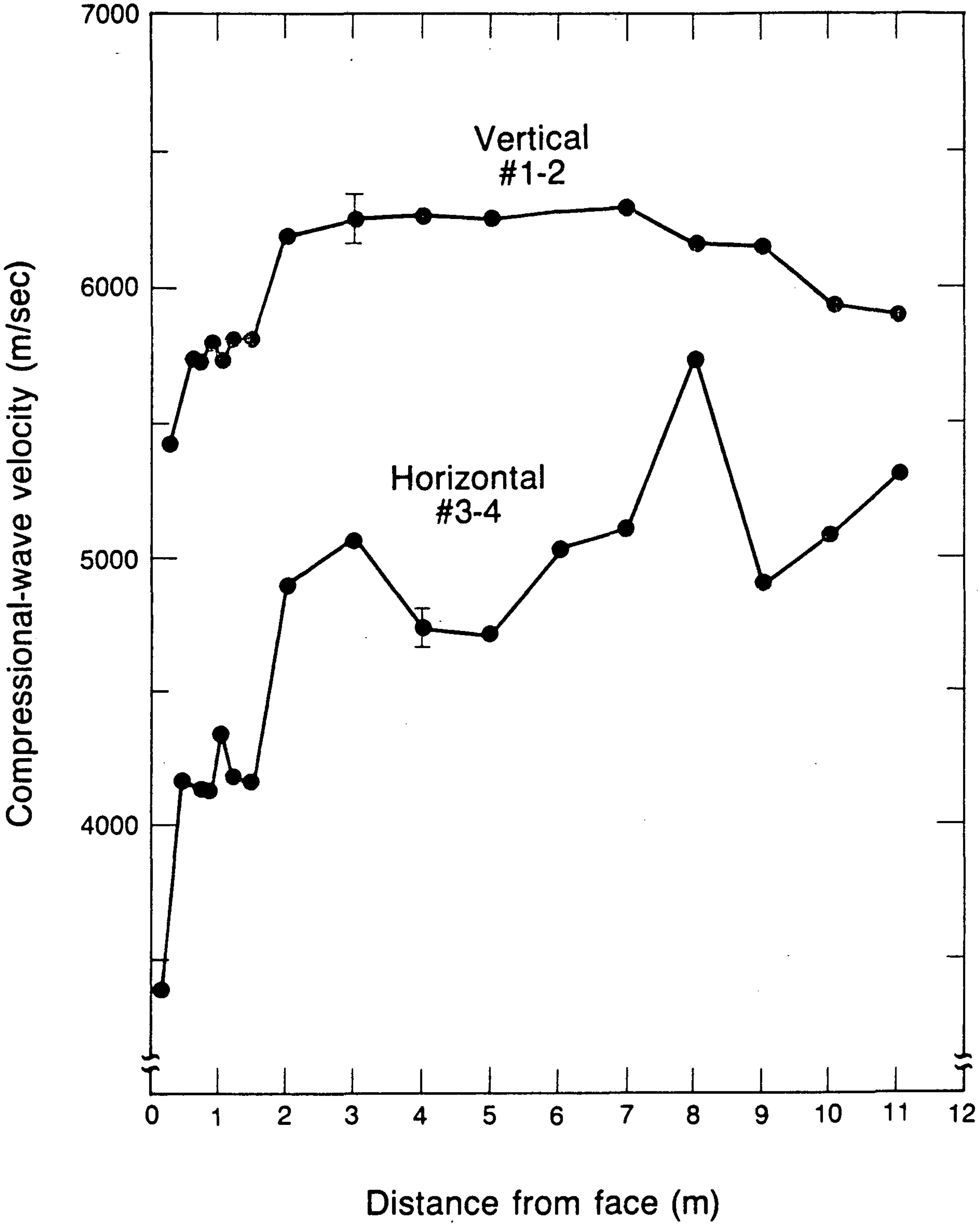
7000
6000
5000
4000
Compressional-wave velocity (m/sec)
Vertical
#1-2
Horizontal
#3-4
0
1
2
3
4
5
6
7
8
9
10
11
12
Distance from face (m)

Figure 3

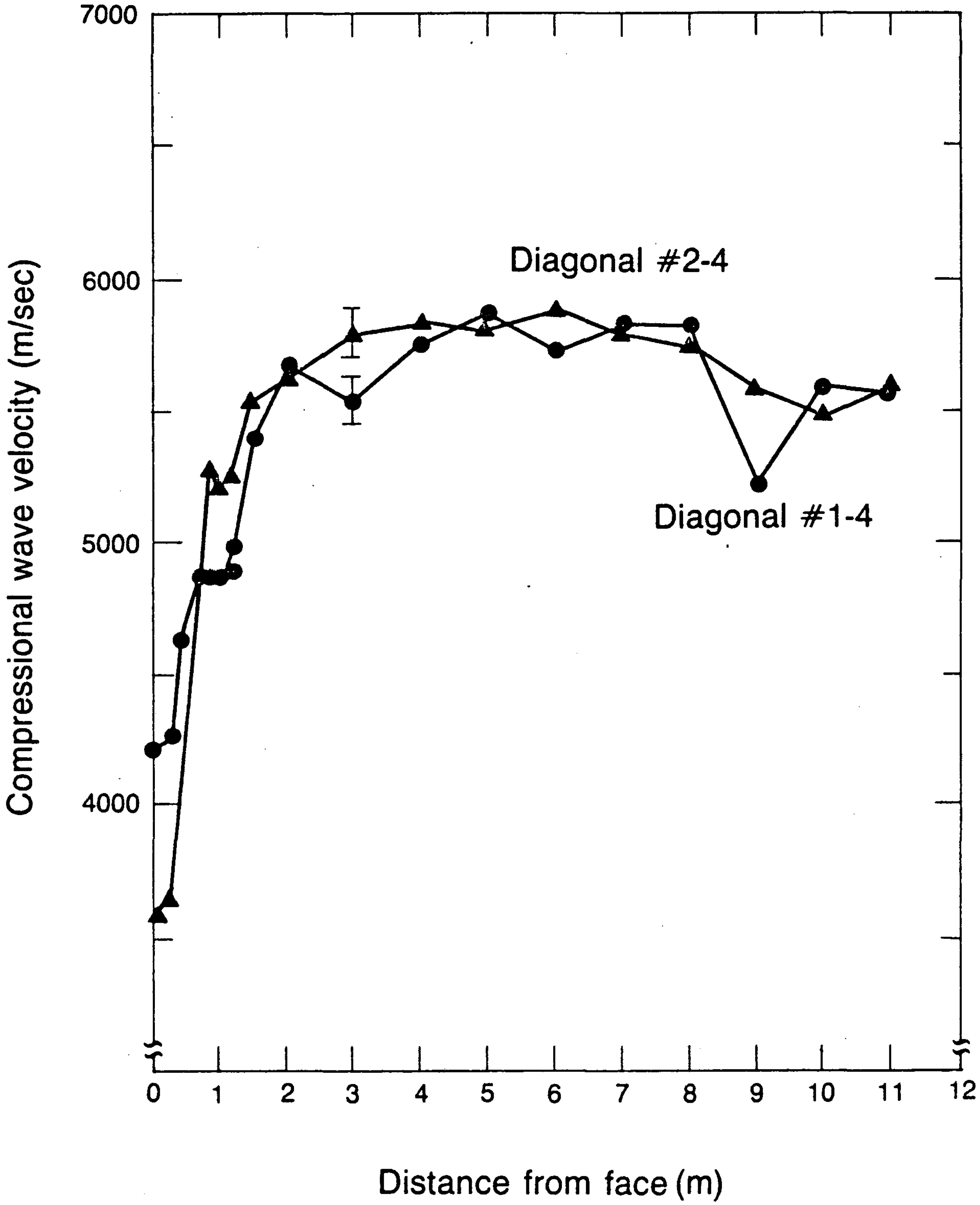
7000
6000
5000
4000
Compressional wave velocity (m/sec)
Diagonal #2-4
Diagonal #1-4
0
1
2
3
4
5
6
7
8
9
10
11
12
Distance from face (m)

Figure 4

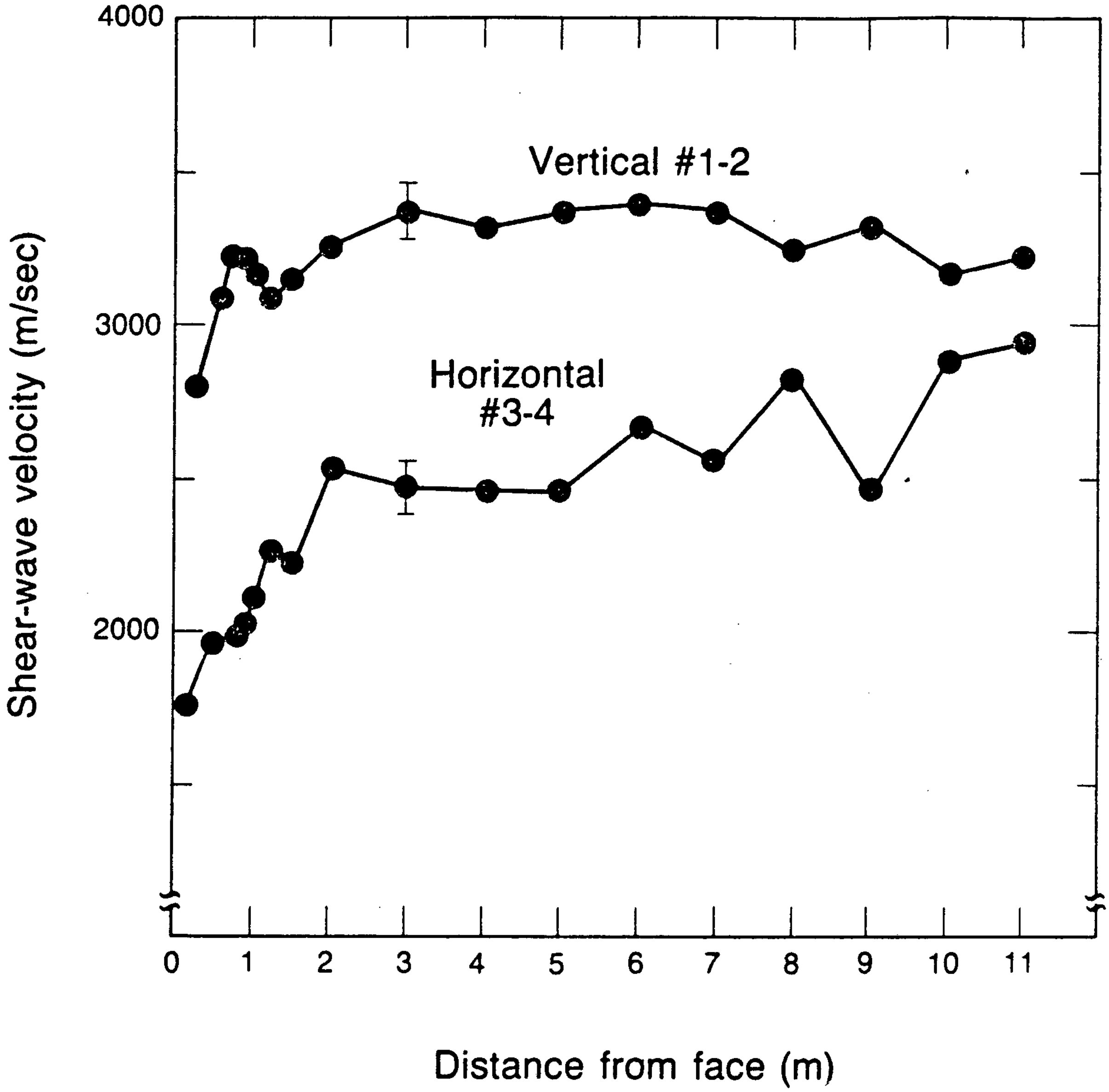
4000
3000
2000
Shear-wave velocity (m/sec)
Vertical #1-2
Horizontal
#3-4
0
1
2
3
4
5
6
7
8
9
10
11
Distance from face (m)

Figure 5

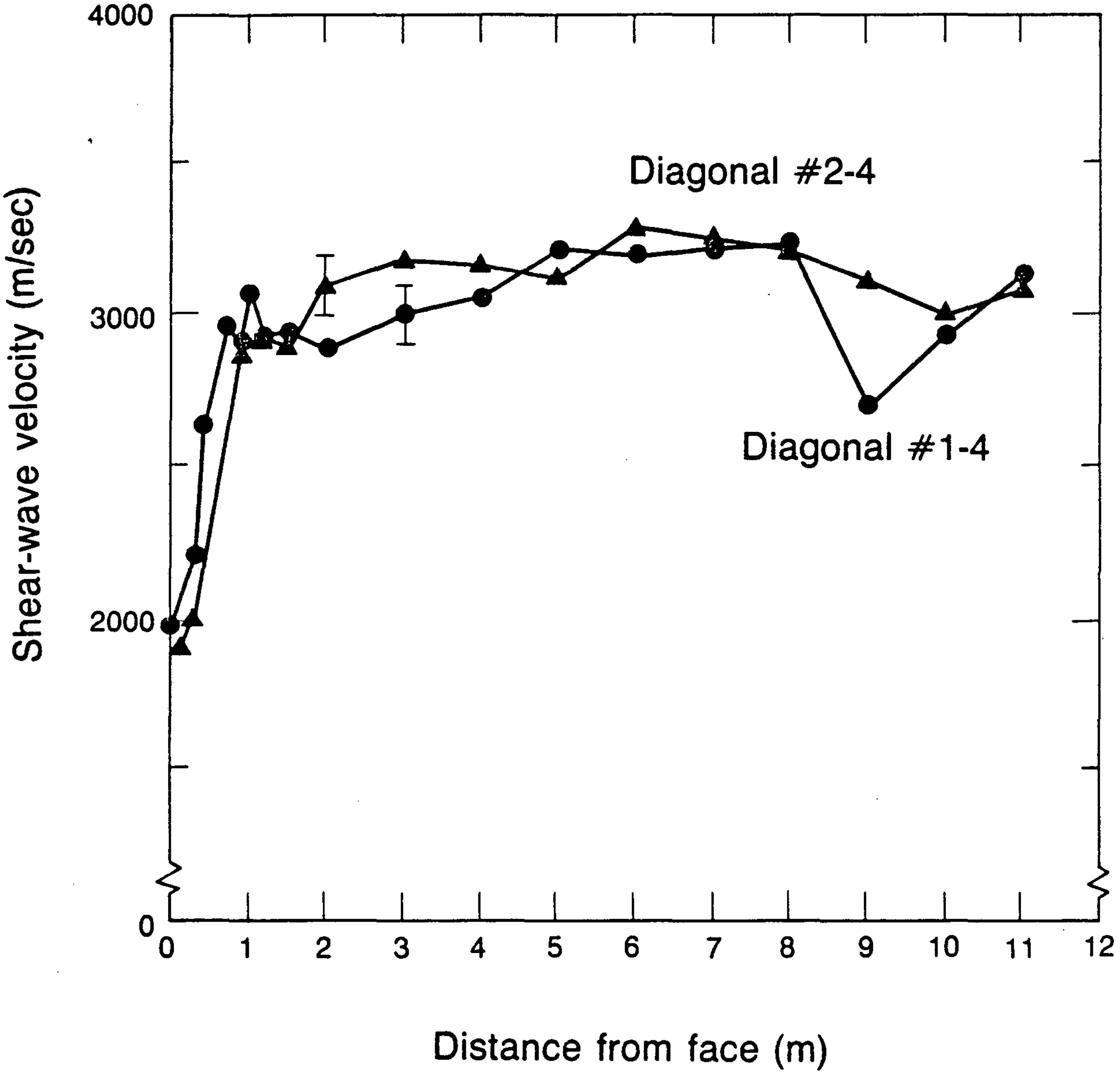
4000
3000
2000
0
Shear-wave velocity (m/sec)
Diagonal #2-4
Diagonal #1-4
0
1
2
3
4
5
6
7
8
9
10
11
12
Distance from face (m)

Figure 6

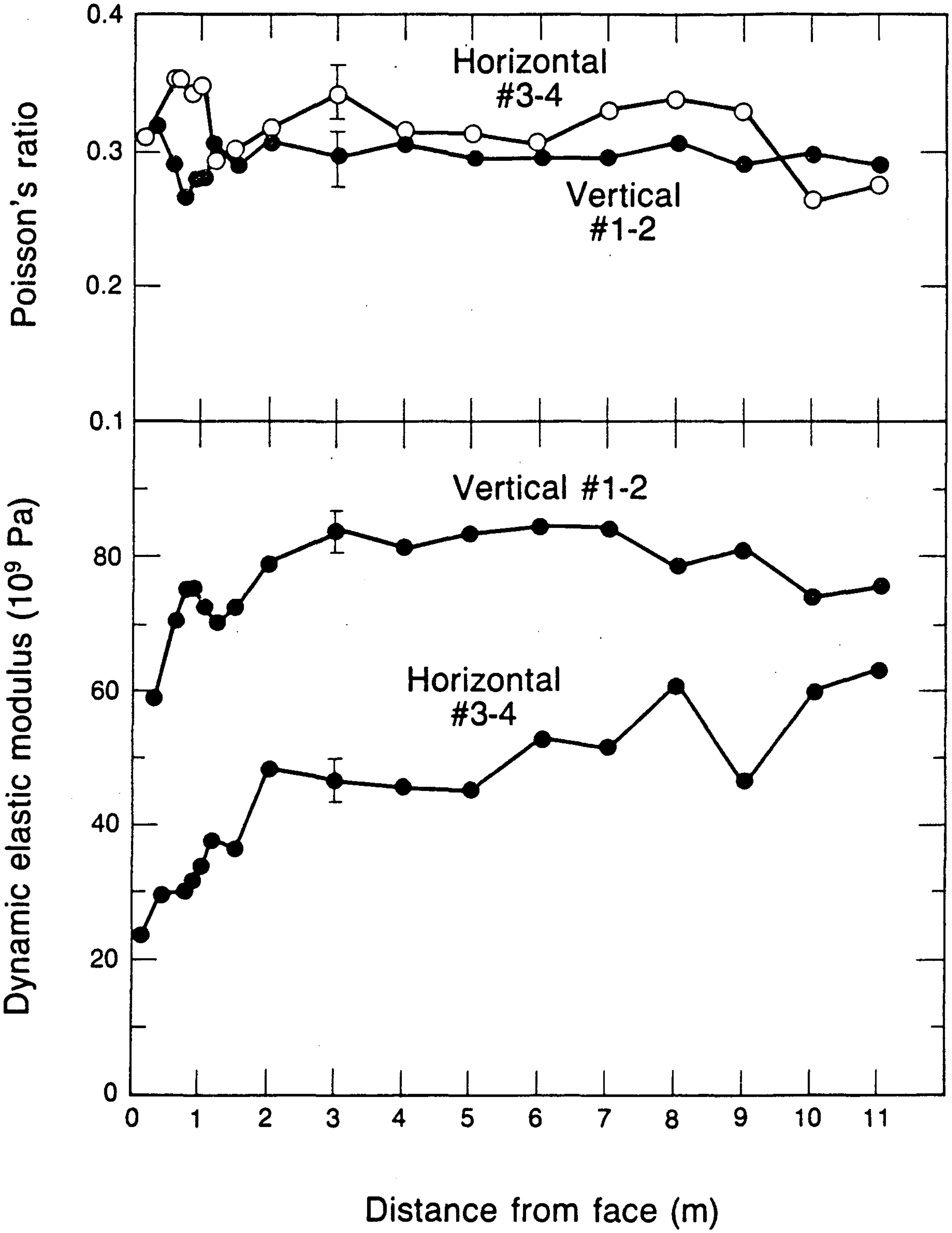
Poisson's ratio
0.4
0.3
0.2
0.1
Horizontal
#3-4
Vertical
#1-2
Dynamic elastic modulus (10^9 Pa)
Vertical #1-2
Horizontal
#3-4
0
20
40
60
80
0
1
2
3
4
5
6
7
8
9
10
11
Distance from face (m)

Figure 7

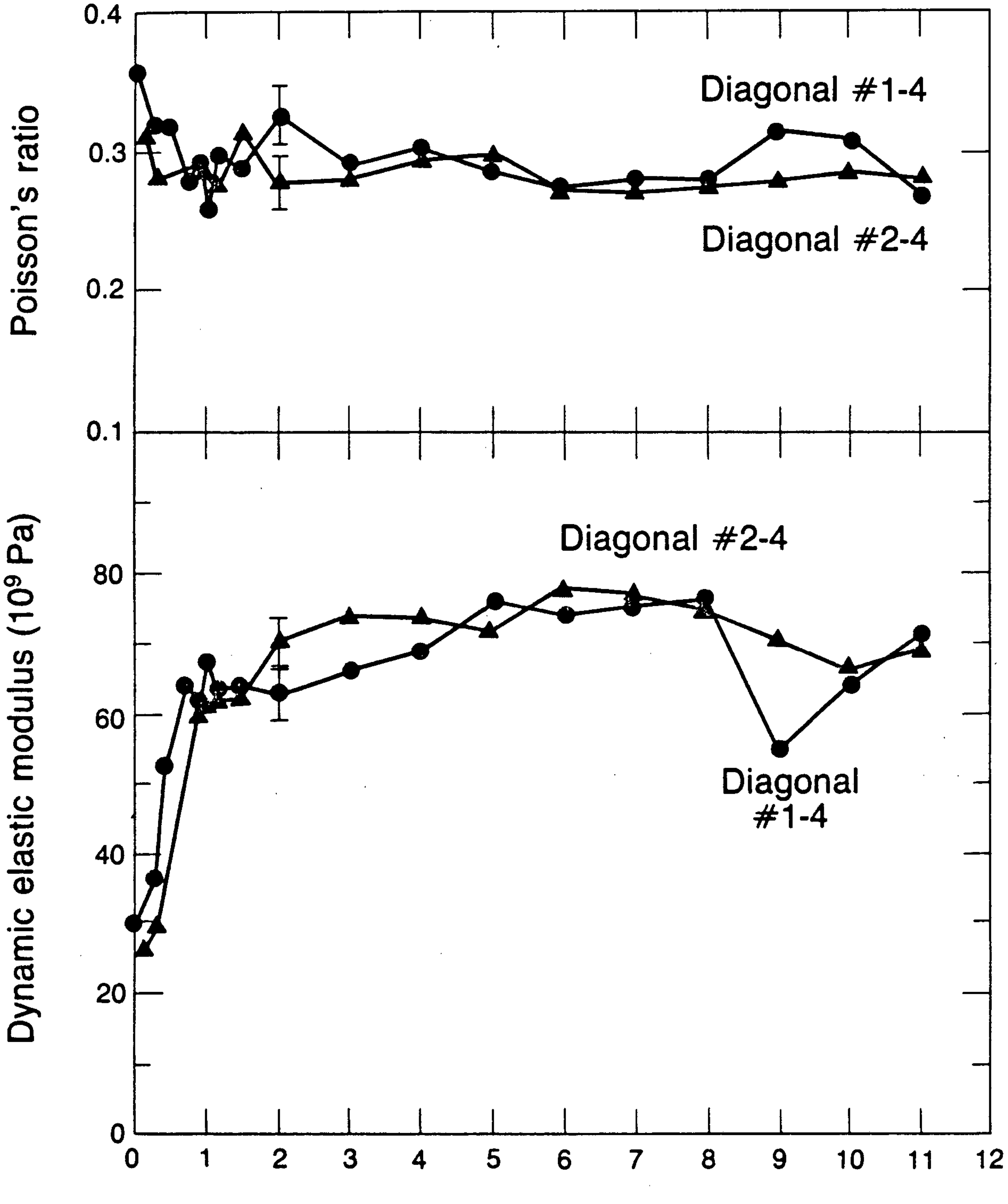
0.4
0.3
0.2
0.1
Poisson's ratio
Diagonal #1-4
Diagonal #2-4
Dynamic elastic modulus (10⁹ Pa)
80
60
40
20
0
Diagonal #2-4
Diagonal #1-4
0
1
2
3
4
5
6
7
8
9
10
11
12
Distance from face (m)

Figure 8

TECHNICAL INFORMATION DEPARTMENT
LAWRENCE BERKELEY LABORATORY
UNIVERSITY OF CALIFORNIA
BERKELEY, CALIFORNIA 94720